

# A New Absolute Nodal Coordinate Formulation of Solid Element with Continuity Condition and Viscosity Model

Ma Chao<sup>1</sup>, Wang Ran<sup>1</sup>, Wei Cheng<sup>1</sup>, Zhao Yang<sup>1</sup>

*1 Department of Aerospace Engineering  
Harbin Institute of Technology  
Harbin, 150001, China*

**Abstract** — In multibody system dynamics formulations, the modeling of classical non-isoparametric element cannot accurately describe the deformation of cross sections. Unlike the conventional methods, the absolute nodal coordinate formulation (ANCF) of solid element is not only able to achieve section description, but also can directly describe the section deformation through the node coordinates. But the deficiency of incomplete polynomial using the current ANCF solid element is expected to avoid locking problems that cannot conform to the derivative coordinates across the boundary. In this paper, the ANCF solid element with continuity condition and internal viscoelastic damping has been provided and achieved. The continuity condition could be applied to make the neighboring elements achieve continuity across boundary, and the viscosity model of the ANCF solid element is proposed for large deformations. Some numerical simulations are provided and according to the comparative results, the ANCF solid element can get higher accuracy than traditional finite element and former ANCF element.

**Keywords** - multibody system dynamics; absolute nodal coordinate formulation; large deformation; continuity condition; internal damping model

## I. INTRODUCTION

For the current multibody system dynamics, the modeling of classical non-isoparametric beam elements is mainly based on the Euler-Bernoulli and Timoshenko beam theory, which cannot accurately describe the deformation of the beam cross section [1]. The ANCF element which was first proposed and reported by Shabana [2] is able to achieve section describe, but it is necessary to introduce additional description frames and deal with a series of locking problems [3-5]. Olshevskiy [6] proposed a solid element based on Shabana's ANCF element. Different from the elements mentioned above, the Olshevskiy's ANCF solid element directly describes the section deformation through the node coordinates without bringing in additional coordinates and the locking problems can also be avoided by using the incomplete interpolation function which used to describe the displacement field. Based on the Olshevskiy's solid element, the ANCF solid element considering the continuity condition and internal viscoelastic damping has been provided and achieved for the first time in this paper. With this solid element, the modeling of a rotating flexible beam is realized. According to numerical simulations, it is able to get some nonlinearity results with solid element and the precision is much higher than traditional finite element and former ANCF element.

In this paper, the total Lagrangian finite element approach for ANCF solid element using continuum mechanics is proposed in section 2.1 in chapter 2. The continuity condition of the ANCF solid element and the viscoelastic damping model which derived from the Kelvin-Voigt model are developed in section 2.2 and 2.3. The system dynamics equations are proposed in section 2.4. In

chapter 3, some typical simulations are represented using the ANCF solid element. Finally, the conclusions are summarized and its further studies are forecasted in chapter 4.

## II. REPRESENTATION OF THE ANCF SOLID ELEMENT

The ANCF solid element is a Lagrangian finite element, using the absolute nodal coordinate as the generalized coordinate, which was proposed to handle the large deformations in flexible problems in recent years. The following derivations of the finite element model for the ANCF solid element are based on the continuum mechanics theory and finite element method.

### A. Displacement Field

In the reference configuration, the global position vector of an arbitrary point on the element can obtain by using the global shape function and element absolute nodal coordinates. The relationship can be written as follows [7-8]:

$$\mathbf{r} = \mathbf{S}(x, y, z) \mathbf{e}(t) \quad (1)$$

where  $\mathbf{S}$  is the shape function matrix that depends on the element spatial coordinates in global coordinate;  $x$ ,  $y$  and  $z$  are the node position coordinates in the local coordinate;  $\mathbf{e}$  is the vector of time-dependent nodal coordinates that define the displacements and derivatives at a set of nodal points selected for the element.

Assume the dimensions of the solid element are  $a \times b \times c$  and the element has 8 nodes, so the nodal coordinates  $\mathbf{e}$  at the node  $k$  of the finite element  $j$  can be defined as:

$$\mathbf{e}^{jk} = [\mathbf{r}^{jk^T} \ \mathbf{r}_x^{jk^T} \ \mathbf{r}_y^{jk^T} \ \mathbf{r}_z^{jk^T}]^T \quad k = 1, \dots, 8 \quad (2)$$

where  $r^{jk}$  is the absolute position vector at the node  $k$  of the finite element  $j$ , and  $r_x^{jk}$ ,  $r_y^{jk}$  and  $r_z^{jk}$  are the position gradients vectors obtained by differentiation with respect to the spatial coordinates  $x$ ,  $y$  and  $z$ . Clearly, the proposed element has 32 coordinates and 96 degrees of freedom. The ANCF solid element is shown in Fig. 1.

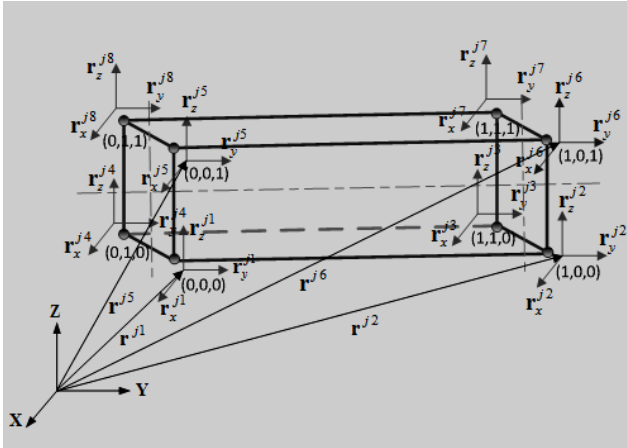


Figure 1. The Solid element

The displacement field of solid element can be defined using a polynomial with 32 coordinates as:

$$\begin{aligned} \phi(x, y, z) = & \alpha_1 + \alpha_2 x + \alpha_3 y + \alpha_4 z + \alpha_5 x^2 + \alpha_6 y^2 + \\ & \alpha_7 z^2 + \alpha_8 xy + \alpha_9 yz + \alpha_{10} xz + \alpha_{11} x^3 + \\ & \alpha_{12} y^3 + \alpha_{13} z^3 + \alpha_{14} x^2 y + \alpha_{15} x^2 z + \\ & \alpha_{16} y^2 z + \alpha_{17} xy^2 + \alpha_{18} xz^2 + \alpha_{19} yz^2 + \\ & \alpha_{20} xyz + \alpha_{24} x^3 y + \alpha_{25} x^3 z + \alpha_{26} xy^3 + \\ & \alpha_{27} y^3 z + \alpha_{28} xz^3 + \alpha_{29} yz^3 + \alpha_{30} x^2 yz + \\ & \alpha_{31} xy^2 z + \alpha_{32} xyz^2 + \alpha_{36} x^3 yz + \\ & \alpha_{37} xy^3 z + \alpha_{38} xyz^3 \end{aligned} \quad (3)$$

where  $\alpha_k$  are the polynomial coefficients, and  $x^4$ ,  $y^4$ ,  $z^4$ ,  $x^2 y^2$ ,  $y^2 z^2$ ,  $z^2 x^2$  are ignored as the redundancy terms. As a result, the equation in Equation 3 is an incomplete interpolation polynomial.

According to the absolute nodal coordinate vector  $e$  and displacement interpolation function  $\phi(x, y, z)$ , the components of the shape function matrix of the ANCF solid element can be derived as follows:

$$\begin{cases} S^{k,1} = (-1)^{1+\xi_k+\eta_k+\zeta_k} (\xi + \xi_k - 1) \cdot \\ \quad (\eta + \eta_k - 1)(\zeta + \zeta_k - 1) \cdot \\ \quad (1 + (\xi - \xi_k)(1 - 2\xi) + \\ \quad (\eta - \eta_k)(1 - 2\eta) + \\ \quad (\zeta - \zeta_k)(1 - 2\zeta)) \\ S^{k,2} = (-1)^{\eta_k+\zeta_k} a \xi^{\xi_k+1} (\xi - 1)^{2-\xi_k} \cdot \quad k = 1, \dots, 8 \quad (4) \\ \quad \eta^{\eta_k} (\eta - 1)^{1-\eta_k} \zeta^{\zeta_k} (\zeta - 1)^{1-\zeta_k} \\ S^{k,3} = (-1)^{\xi_k+\zeta_k} b \zeta^{\zeta_k} (\xi - 1)^{1-\xi_k} \eta^{\eta_k+1} \cdot \\ \quad (\eta - 1)^{2-\eta_k} \zeta^{\zeta_k} (\zeta - 1)^{1-\zeta_k} \\ S^{k,4} = (-1)^{\xi_k+\eta_k} c \xi^{\xi_k} (\xi - 1)^{1-\xi_k} \eta^{\eta_k} \cdot \\ \quad (\eta - 1)^{1-\eta_k} \zeta^{\zeta_k+1} (\zeta - 1)^{2-\zeta_k} \end{cases}$$

where  $a$ ,  $b$  and  $c$  are the dimensions of the element along the axis  $x$ ,  $y$  and  $z$ ,  $\xi_k$ ,  $\eta_k$  and  $\zeta_k$  are the dimensionless coefficients at node  $k$ ,  $\xi = x/a$ ,  $\eta = y/b$ ,  $\zeta = z/c$ . The position vector of an arbitrary material point on element  $j$  can be written as:

$$r^j = \sum_{k=1}^8 [S^{k,1} I_{3 \times 3} \quad S^{k,2} I_{3 \times 3} \quad S^{k,3} I_{3 \times 3} \quad S^{k,4} I_{3 \times 3}] e^{jk} \quad (5)$$

where  $S^j$  and  $e^j$  are, respectively, the element global shape function matrix and the vector of nodal coordinates.

### B. Continuity Condition

In previous section, an incomplete interpolation polynomial is used to describe the displacement field of the element. But due to the deficient of the incomplete polynomial using in the ANCF solid element cannot conformal in the derivative coordinates across the boundary. It leads to the presence of higher-order continuous inconsistency at element boundary. As a result, it is necessary to consider the issue of continuity between the elements in order to guarantee the modeling accuracy when using multiple elements.

The definition of continuity between two adjacent elements is shown in Figure. 2, where the Arabic numeral is the element node number, superscript is the element number, and subscript is the material derivative in corresponding direction.

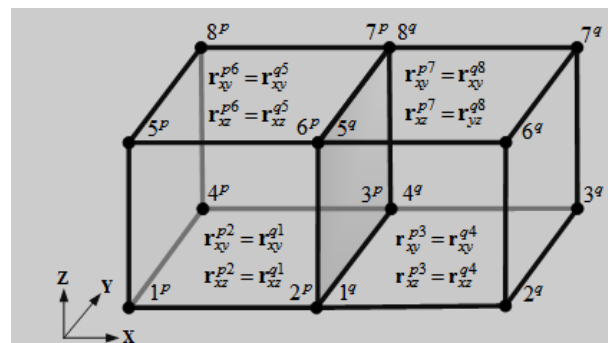


Figure 2. Continuity between adjacent elements

The ANCF solid element meets the  $C^1$  continuous at each node by definition, for it uses the positions and the derivative of positions as the nodal coordinates. Clearly, the nodes on the adjacent surface between element  $p$  and  $q$  meet the  $C^0$ ,  $C_y^1$  and  $C_z^1$  continuous. The  $C_x^1$  continuous needs to satisfy the following equation in order to guarantee the multi-element continuously:

$$\mathbf{S}_x(\xi=1)\mathbf{e}^p = \mathbf{S}_x(\xi=0)\mathbf{e}^q \quad (6)$$

where  $\mathbf{S}_x$  is the derivative of element shape function  $\mathbf{S}$  in  $x$  direction, and  $\mathbf{e}$  is the vector of time-dependent nodal coordinates. The Equation 6 can be rewritten as

$$\begin{cases} \mathbf{r}_{xy}^{pm} = \mathbf{r}_{xy}^{qn} \\ \mathbf{r}_{xz}^{pm} = \mathbf{r}_{xz}^{qn} \end{cases} \quad m=2,3,6,7 \quad n=1,4,5,8 \quad (7)$$

where  $\mathbf{r}_{xy}^{pm}$  is the partial derivatives of the node  $m$  from the element  $p$  along  $x$  and  $y$  directions,  $m$  and  $n$  are, respectively, the sharing node on the adjacent surface between element  $p$  and  $q$ .

### C. Constitutive Equations

The ANCF solid element proposed by Olshevskiy [6] used linear elastic model and ignored the effect of damping on the dissipation of energy in deformation. In the modeling of solid element in this paper, according to the Kelvin-Voigt model [9], the viscoelastic model for ANCF solid element suitable for large deformation is established. The total stresses for isotropic homogeneous viscoelastic material can be written as the sum of the elastic stress due to the deformation and the stress due to the damping, that is,

$$\boldsymbol{\sigma}_k = \boldsymbol{\sigma}_{ke} + \boldsymbol{\sigma}_{kd} \quad (8)$$

Where  $\boldsymbol{\sigma}_k$  is the element stress,  $\boldsymbol{\sigma}_{ke}$  and  $\boldsymbol{\sigma}_{kd}$  are, respectively, the elastic stress and the stress due to damping.

Describe the strain using the Green-Lagrange strain tensor in reference configuration as follows:

$$\boldsymbol{\varepsilon} = \frac{1}{2}(\mathbf{J}^T \mathbf{J} - \mathbf{I}) \quad (9)$$

Where  $\boldsymbol{\varepsilon}$  is Green-Lagrange strain tensor, and  $\mathbf{J}$  is deformation gradient represented by  $\mathbf{J} = [\mathbf{r}_x \quad \mathbf{r}_y \quad \mathbf{r}_z]$ . Rewrite the Equation 9 to a vector form as follows:

$$\boldsymbol{\varepsilon}_v = \frac{1}{2} \left[ \mathbf{r}_x^T \mathbf{r}_x - 1 \quad \mathbf{r}_y^T \mathbf{r}_y - 1 \quad \mathbf{r}_z^T \mathbf{r}_z - 1 \quad \mathbf{r}_x^T \mathbf{r}_y \quad \mathbf{r}_x^T \mathbf{r}_z \quad \mathbf{r}_y^T \mathbf{r}_z \right]^T \quad (10)$$

where the subscript  $v$  represents the vector form of the tensor. In reference configuration, describe the elastic stress using the second Piola-Kirchhoff stress tensor as follows:

$$\boldsymbol{\sigma}_{p2} = \mathbf{J} \mathbf{J}^{-1} \boldsymbol{\sigma} \mathbf{J}^{-1^T} \quad (11)$$

where  $\boldsymbol{\sigma}_{p2}$  is the second Piola-Kirchhoff stress tensor, and  $\mathbf{J}$  is the determinant of deformation gradient represented as  $\mathbf{J} = \mathbf{r}_x \cdot (\mathbf{r}_y \times \mathbf{r}_z)$ , and  $\boldsymbol{\sigma}$  is Cauchy stress tensor in current configuration.

According to the generalized Hooke's law, the relationship of strain and stress are,

$$\boldsymbol{\sigma}_{p2,v} = \mathbf{E} \boldsymbol{\varepsilon}_v \quad (12)$$

where  $\mathbf{E}$  is material coefficients matrix represented as follows which can be determined by constitutive relations:

$$\mathbf{E} = \frac{E}{(1+\nu)(1-2\nu)} \begin{bmatrix} 1-\nu & \nu & \nu & 0 & 0 & 0 \\ \nu & 1-\nu & \nu & 0 & 0 & 0 \\ \nu & \nu & 1-\nu & 0 & 0 & 0 \\ 0 & 0 & 0 & 1-2\nu & 0 & 0 \\ 0 & 0 & 0 & 0 & 1-2\nu & 0 \\ 0 & 0 & 0 & 0 & 0 & 1-2\nu \end{bmatrix} \quad (13)$$

Where  $E$  is elastic modulus, and  $\nu$  is Poisson's ratio. The elastic strain energy can be expressed as follows:

$$U_{ke} = \frac{1}{2} \int_V \boldsymbol{\sigma}_{p2} : \boldsymbol{\varepsilon} \, dV \quad (14)$$

Define the relationship between damping stress and the rate of change of the strain tensor as follows:

$$\boldsymbol{\sigma}_{d,v} = \mathbf{D} \dot{\boldsymbol{\varepsilon}}_v \quad (15)$$

where  $\boldsymbol{\sigma}_d$  is damping stress, and  $\dot{\boldsymbol{\varepsilon}}$  is the rate of change of the Green-Lagrange strain tensor.  $\mathbf{D}$  is material damping coefficients matrix determined by constitutive equation and could be represented by matrix as follows:

$$\mathbf{D} = \begin{bmatrix} \lambda_v + 2\mu_v & \lambda_v & \lambda_v & 0 & 0 & 0 \\ \lambda_v & \lambda_v + 2\mu_v & \lambda_v & 0 & 0 & 0 \\ \lambda_v & \lambda_v & \lambda_v + 2\mu_v & 0 & 0 & 0 \\ 0 & 0 & 0 & 2\mu_v & 0 & 0 \\ 0 & 0 & 0 & 0 & 2\mu_v & 0 \\ 0 & 0 & 0 & 0 & 0 & 2\mu_v \end{bmatrix} \quad (16)$$

where  $\lambda_v$  and  $\mu_v$  are the coefficients defined as  $(E\gamma_{di} - 2G\gamma_{de}(1-2\nu))/3(1-2\nu)$ ,  $\mu_v = G\gamma_{de}$ , and  $G$  is the shearing modulus.  $\gamma_{di}$  and  $\gamma_{de}$  are, respectively, the dissipation factors associated with the dilatational and deviatoric stresses. The dissipation power can be written as follows:

$$P_{kd} = \frac{1}{2} \int_V \boldsymbol{\sigma}_d : \dot{\boldsymbol{\varepsilon}} \, dV \quad (17)$$

Substitute Equation 12 and 15 into Equation 8, the solid element constitutive equation described by the elasticity coefficients and damping coefficients can be written as:

$$\boldsymbol{\sigma}_{k,v} = \mathbf{E} \boldsymbol{\varepsilon}_v + \mathbf{D} \dot{\boldsymbol{\varepsilon}}_v \quad (18)$$

The Equation 18 is the viscoelastic constitutive equation with absolute nodal coordinates description of solid element. In the derivation, Green-Lagrange strain tensor is directly used to deduce the strain energy without introducing deformation assumptions, so the geometric nonlinearity is preserved. It makes the ANCF solid element can describe the large deformation and large rotation directly without introducing additional descriptions.

### D. Dynamics Equations

For the viscoelastic material, assuming that  $V$  and  $\nu$  are, respectively, the volume of element before and after the deformation, and the corresponding density are  $\rho$  and  $\rho_0$ .

According to the principle of virtual work, the elastic force of element in reference configuration can be obtained by Green-Lagrange strain tensor and the second Piola-Kirchhoff stress tensor as follows:

$$\delta W_{ke}^j = -\int_V \sigma_{p2}^j : \delta \varepsilon^j dV = -\underline{Q}_{ke}^j \cdot \delta e^j \quad (19)$$

where  $\delta W_{ke}^j$  is the virtual work of elastic force, and  $\underline{Q}_{ke}^j$  is generalized elastic force.

For damping force, it can be obtained from the rate of change of the Green-Lagrange strain tensor and damping stress as follows:

$$\delta W_{kd}^j = -\left(\int_V \sigma_d^j : \delta \dot{\varepsilon}^j dV\right) dt = -\underline{Q}_{kd}^j \cdot \delta e^j \quad (20)$$

where  $\delta W_{kd}^j$  is the virtual work of damping force, and  $\underline{Q}_{kd}^j$  is generalized damping force.

In addition to the virtual work of the elastic force and damping force, the principle of virtual work also defines the virtual works of the inertia and applied forces. The virtual work of the inertia forces is defined as

$$\delta W_I^j = \int_V \rho_0 \mathbf{a}^{jT} \cdot \delta \mathbf{r}^j dV = \underline{Q}_I^j \cdot \delta e^j = \mathbf{M}^j \ddot{e}^j \cdot \delta e^j \quad (21)$$

where  $\delta W_I^j$  is the virtual work of inertial force, and  $\mathbf{a}^j$  is acceleration vector of element  $j$ ,  $\underline{Q}_I^j$  is generalized inertial force,  $\mathbf{M}^j$  is a constant symmetric mass matrix of element  $j$ ,  $\mathbf{M}^j = \int_V \rho_0 \mathbf{S}^{jT} \mathbf{S}^j dV$ .

For the external force, it can be obtained by principle of virtual work as follows:

$$\delta W_e^j = \int_V \mathbf{f}^{jT} \cdot \delta \mathbf{r}^j dV = \underline{Q}_e^j \cdot \delta e^j \quad (22)$$

where  $\delta W_e^j$  is the virtual work of external force,  $\mathbf{f}^j$  is external force, and  $\underline{Q}_e^j$  is generalized external force.

According to Equation 19-22, the motion equation of element  $j$  in the unconstrained case can be written as:

$$\mathbf{M}^j \ddot{e}^j + \underline{Q}_{ke}^j + \underline{Q}_{kd}^j - \underline{Q}_e^j = \mathbf{0} \quad (23)$$

The dynamics equation of multibody system is written as:

$$\delta \mathbf{q}^T (\mathbf{M} \ddot{\mathbf{q}} + \mathbf{C}_q^T \boldsymbol{\lambda} - \mathbf{Q}) = 0 \quad (24)$$

where  $\mathbf{M}$  is mass matrix of the system, can be obtained by Equation 21,  $\mathbf{q}$  is generalized coordinate of the system, can be obtained by Equation 2,  $\mathbf{C}_q$  is the matrix of constraint equation,  $\boldsymbol{\lambda}$  is the vector of Lagrange multipliers,  $\mathbf{Q}$  is the generalized force of the system, including the elastic force  $\underline{Q}_{ke}$ , the damping force  $\underline{Q}_{kd}$  and the external force  $\underline{Q}_e$ , which can be respectively obtained by Equation 19, 20 and 22.

### III. NUMERICAL EXAMPLES

In this part, both simple pendulum and double pendulum are used to demonstrate the application of the ANCF solid element with continuity condition and viscosity model developed in this investigation. As a comparison, the traditional finite element from the finite element analysis

software and former ANCF element from literature are used as the comparative analysis.

#### A. Simple Pendulum

The beam is oriented horizontally along  $x$  direction with the constrained by spherical joints at the end of one side. The dimensions of beam are  $1.0 \text{ m} \times 0.02 \text{ m} \times 0.02 \text{ m}$ , and the dimensions of ANCF solid element are  $0.25 \text{ m} \times 0.02 \text{ m} \times 0.02 \text{ m}$ , adding the  $C^1$  continuity conditions between the elements. The density of the material  $\rho = 7200 \text{ kg/m}^3$ . The gravity acceleration  $g = 9.8 \text{ m/s}^2$ . The modulus of elasticity  $E = 2.0 \times 10^8 \text{ Pa}$ . The Poisson's ratio  $\nu = 0.3$ . The dissipation factors  $\gamma_{di} = 0.5 \times 10^{-5}$ ,  $\gamma_{de} = 0.3 \times 10^{-6}$ . The beam is in a static at the initial and rotates freely under the gravity when the simulation begins. Use the BEAM189 element form the ANSYS software to set up a rotating beam simulation at the same conditions. Compare the results between the ANCF solid element and BEAM189 element to obtain the displacement curves as shown in Figure 3.

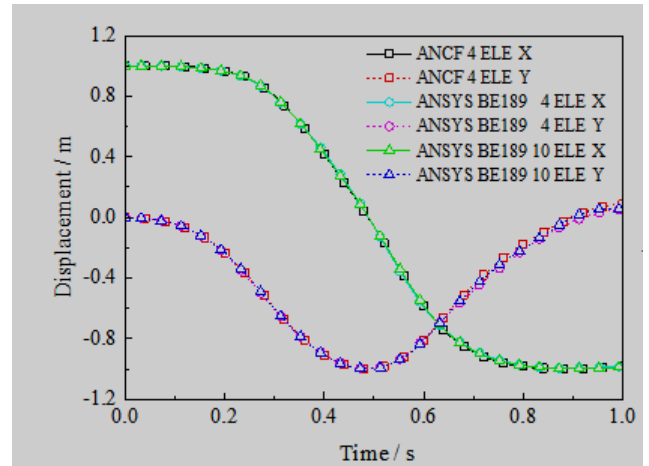
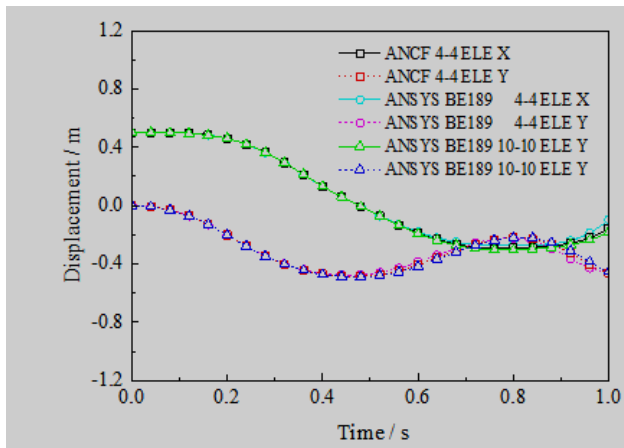


Figure 3. Comparison of displacement of the high stiffness beam at the end point

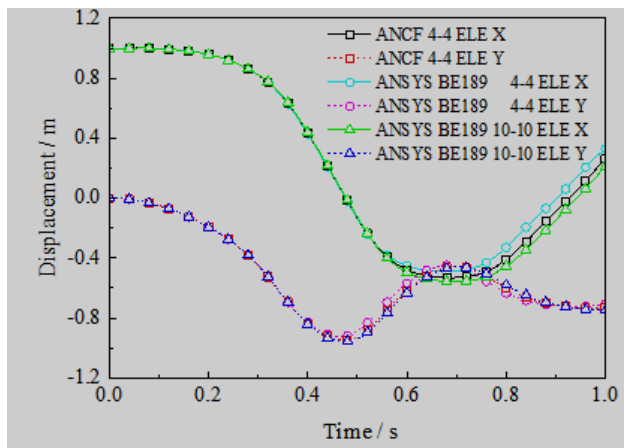
From the Figure 3 we can see that, in high stiffness case, the displacement curves obtained by 4 ANCF solid elements are almost identical with curves obtained by 4 and 10 BEAM189 elements, which illustrate that the capacity of the ANCF solid element in dealing with small deformations is equal to the traditional element and the two methods maintain a fine consistency.

#### B. Double Pendulum

In this case, a double pendulum is set up based on the simple pendulum discussed in the previous section. The modulus of elasticity  $E = 2.0 \times 10^7 \text{ Pa}$  for both upper and lower beam, and all other conditions maintain consistent. The displacements at the end points from the upper and lower beam in first rotary using the ANCF solid element and ANSYS BEAM189 element are compared in Fig. 4.



(a) The displacement curves of upper beam.



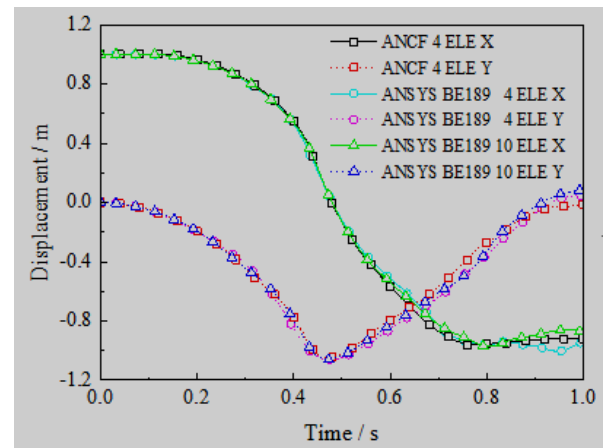
(b) The displacement curves of lower beam

Figure 4. Comparison of displacement of the beams at the end points.

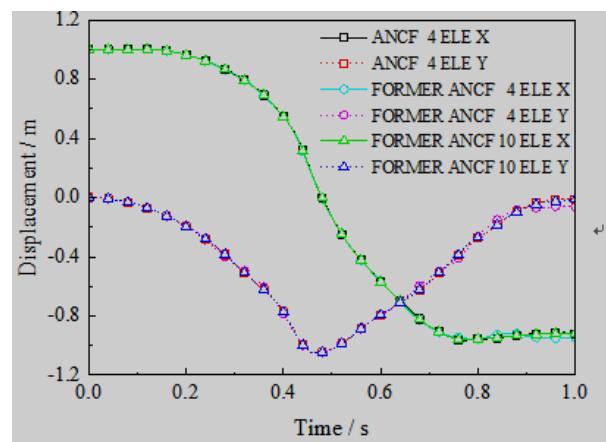
The difference of the displacement curves plotted in Fig. 4 shows that, as the beam stiffness decreased, the flexible deformation is increased. The advantages of ANCF solid element are gradually embodied. When the double pendulum begins to rotate, the displacement curves obtained by 4 ANCF solid elements and curves obtained by 4 and 10 BEAM189 elements are almost identical at the initial time. With the increase of the flexible deformation, the curves of 10 BEAM189 elements deviate from the curves of 4 BEAM189 elements, which illustrate that the number of elements has important implications on the modeling accuracy. That means the curves of 10 BEAM189 elements have higher precision and better reflection for deformations than 4 BEAM189 elements. On the other side, the curves of 10 BEAM189 elements approach to the curves of ANCF solid elements gradually. Although the traditional element can compensate the accuracy by increasing the number of elements, they cannot solve the large deformation problems fundamentally. However, the ANCF solid element show a good adaptive ability and high accuracy for describe the deformation of the flexible beam.

C. Large Deformation Pendulum

The following simulation considers large flexible condition in order to verify the applicability of the ANCF solid element. The modulus of elasticity  $E = 2.0e6$  Pa, and all other conditions maintain consistent. The displacements at the end point of low stiffness beam in first rotary using the ANCF solid element and ANSYS BEAM189 element are shown in Figure. 5(a), and the displacements at the end point using the ANCF solid element and former ANCF solid element from literature [6] are shown in Fig. 5(b).



(a) Curves of ANCF solid elements and BEAM189 elements.



(b) Curves of ANCF solid elements and former ANCF elements

Figure 5. Comparison of displacement of the low stiffness beam at the end point

The difference of the displacement curves shown in Fig. 5(a) show that, as the beam stiffness is low, the flexibility is large, the advantages of ANCF solid element are fully embodied. From the diagrams we can see that, in large flexible case, in a short time after the start of the simulation, the displacement curves obtained by 4 ANCF solid elements and curves obtained by 4 and 10 BEAM189 elements are almost identical. But with the simulation goes on, these curves begin to separate gradually. When the simulation performs at about 0.5s, the displacement curves separate completely and deviations are accumulated over time. This

shows that at this time the traditional element for large deformation calculating has been distorted. And the ANCF element shows a good adaptability and ability to describe the large deformation as described in this investigation and other literatures [10-12]. In Fig. 5(b), the ANCF solid element proposed in this paper and the ANCF element from literature [6] are plotted and compared. Both of them keep a good consistency in the whole time. But at 0.9s-1.0s, the displacement curves of 10 former ANCF elements show more consistent to the curves of 4 ANCF elements than the 4 former ANCF solid elements. This illustrates the ANCF solid element can get higher accuracy than former ANCF element and it is consistent with the modeling theory proposed in the previous chapter.

#### IV. CONCLUSIONS

In this paper, the purpose is to propose a solid element model considering continuity condition and internal viscoelastic damping using the absolute nodal coordinate formulation, which is a reported multibody description for large deformation problems recently. In this model, the continuity condition has been used to apply the algebraic constraint equations to make the neighboring elements achieving continuity at the boundary. Using the relationship between the deformation gradients and the components of the Green-Lagrange strain tensor, the viscoelastic model is developed based on the Kelvin-Voigt model for the ANCF solid element. The feasibility of implementing this solid element is demonstrated using several examples and the results obtained by the solid element are compared with the traditional finite element and the former ANCF element. The comparisons show a good agreement in small deformations and some advantages in large deformations from the element developed in this investigation. The simulations illustrate that as the flexibility increased, the ANCF solid element can get higher accuracy than traditional finite element and former ANCF element. The validations, detailed model and other types of constraints for specific applications would be developed in the following research.

#### ACKNOWLEDGMENT

This work is supported by the National Key Basic Research Program, China (No.2013CB733004), and Natural Scientific Research Innovation Foundation in Harbin Institute of Technology, China (No. HIT.NSRIF. 201515).

#### REFERENCES

- [1] A. A. Shabana, "Flexible multibody dynamics: Review of past and recent developments," *Multibody System Dynamics*, vol.1No.2, pp.189-222, 1997.
- [2] A. A. Shabana, "Definition of the slopes and the finite element absolute nodal coordinate formulation," *Multibody System Dynamics*, vol.1, No.3, pp.339-348, 1997.
- [3] J. Gerstmayr, A. A. Shabana, "Analysis of thin beams and cables using the absolute nodal coordinate formulation," *Nonlinear Dynamics*, 2006, vol.45(1), pp.109-130.
- [4] J. Gerstmayr, M. K. Matikainen, "Analysis of stress and strain in the absolute nodal coordinate formulation," *Mechanics Based Design of Structures and Machines*, vol.34, No.4, pp.409-430, 2006.
- [5] D. Garcia-Vallejo, A. M. Mikkola, J. L. Escalona, "A new locking-free shear deformable finite element based on absolute nodal coordinates," *Nonlinear Dynamics*, vol.50, No.1, pp.249-264, 2007.
- [6] A. Olshevskiy, O. Dmitrochenko, C. W. Kim, "Three-dimensional solid brick element using slopes in the absolute nodal coordinate formulation," *Journal of Computational and Nonlinear Dynamics*, vol.9, No.2, pp.1-10, 2014.
- [7] A. A. Shabana, "Dynamics of multibody systems, 3rd ed.," New York: Cambridge University Press, pp.267-304, 2005.
- [8] A. A. Shabana, "Computational continuum mechanics, 2nd ed.," New York: Cambridge University Press, pp.146-217, 2012.
- [9] A. A. Mohamed, A. A. Shabana, "A nonlinear visco-elastic constitutive model for large rotation finite element formulations," *Multibody System Dynamics*, vol.26, No.1, pp.57-79, 2011.
- [10] R. Y. Yakoub, A. A. Shabana, "Three dimensional absolute nodal coordinate formulation for beam elements: Implementation and applications," *Journal of Mechanical Design*, vol.123, No.4, pp.614-621, 2001.
- [11] S. V. Dombrowski, "Analysis of large flexible body deformation in multibody systems using absolute coordinates," *Multibody System Dynamics*, vol. 8, No.4, pp.409-432, 2002.
- [12] K. S. Kerkkänen, J. T. Sopanen, A. M. Mikkola, "A linear beam finite element based on the absolute nodal coordinate formulation," *Journal of Mechanical Design*, vol.127, No.4, pp.621-630, 2005.